F44 Zeeman effect

Franka Neumann and Nick Striebel
Ruprecht Karl University of Heidelberg

5th February 2021, supervised by Olivera-Nieto, Laura

Abstract

The Zeeman effect describes the splitting of spectral lines in an magnetic field. This splitting is used to determine the Bohr magneton μ_B by observing the Zeeman effect using a Lummer-Gehrcke plate. The result $\mu_B = (9.1 \pm 0.4) \cdot 10^{-24} J/T$ agrees with the literature value 1σ-range. Additionally, the wavelength of the $5^1D_2 \rightarrow 5^1P_1$-transition of the used Cadmium lamp is determined using a Czerny-Turner Spectrometer and a Ne-lamp as reference. With high precision $\lambda = (643.845 \pm 0.010) nm$ is determined, agreeing in the 1σ-area with the literature value. The different polarizations of σ- and π-lines is analysed qualitatively.

I Introduction

The main focus of this experiment is the Zeeman effect. It describes the split/shift of the atomic energy levels in an external magnetic field. To observe this effect a gas-discharge lamp is placed in this external field. The different energy levels of the atoms then can be visualized/measured using spectrometers. In this experiment a Cadmium lamp is used in combination with a Lummer-Gehrcke-plate (to observe the splitting) and a Czerny-Turner-spectrometer (to measure the absolute value of the red Cd-line), the recording of the data is done with a CMOS camera.
It should be mentioned that this experiment was done online (due to the Corona pandemic).

I.1 Zeeman effect

From quantum mechanics it is known, that the electron energy levels for different subshells (i.e. different angular momentum l) are degenerated with the magnetic quantum number m_l, $-l \leq m_l \leq l$. Here, $l_z = m_l \cdot \hbar$ is the quantized component of angular momentum along one specified axis, usually the z-axis. An external magnetic field along this axis lifts the degeneracy by producing an energy shift:

$$\Delta E = \frac{e \cdot \hbar}{2 \cdot m_e} m_l \cdot B = \mu_B \cdot m_l \cdot B \qquad (1)$$

μ_B stands for the Bohr magneton. The semi-classic explanation uses the image of the orbiting electron, inducing a magnetic moment, that interacts with external the magnetic field. A more rigorous explanation can be given by using quantum operators. One should note, that the electronic configuration of Cadmium $[Kr]4d^{10}5s^2$ with full subshells results in a total spin $S = 0$, so all spin effects like LS-coupling can be disregarded.
In this experiment we observe the red Cadmium line, produced by the $5^1D_2 \rightarrow 5^1P_1$-transition. The transition rules are $\Delta m_l = 0$ (π-transitions) or $\Delta m_l = \pm 1$ (σ-transitions). π-emission is only visible in transverse direction (relative to the external magnetic field), linearly polarized with the E-vector parallel to the external field. σ-emissions on the other hand are circularly polarized when

viewed in longitudinal direction and therefore appear in transverse direction as linearly polarized at a 90° angle to the π-emission. This can be verified, using polarisers, waveplates and filters (see Figure 1).

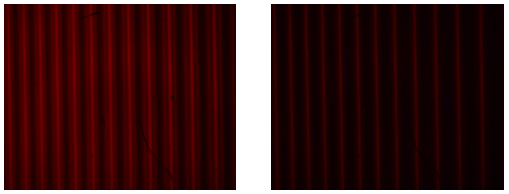

(a) without filter (b) with filter

Figure 1: Effect of polarisation filter in transversal direction

I.2 Lummer-Gehrcke-plate

To resolve the very small shifts in wavelength, a so called Lummer-Gehrcke-plate was used. Considering the geometry of the light path and the condition for constructive interference one finds the following relation between the wavelength shift ($\delta\lambda$) and the displacement of the spectral lines on the camera chip (δa):

$$\delta\lambda = \frac{\delta a}{\Delta a} \cdot \frac{\lambda^2}{2d \cdot \sqrt{n^2 - 1}} \tag{2}$$

In the evaluation a polynomial function for the orders of interference $k = f(a)$ is fitted to reduce the impact of outlier measurements and then locally approximated to first order, so one can insert $\frac{\delta k}{\Delta k} = \frac{\delta a}{\Delta a}$ with $\Delta k = 1$. With the relation for wavelength and photon energy $\Delta E = \frac{hc}{\lambda}$ it follows:

$$\delta E = \begin{cases} \Delta E_\lambda - \Delta E_{\lambda+\delta\lambda} \\ \Delta E_{\lambda-\delta\lambda} - \Delta E_\lambda \end{cases} \approx \frac{hc}{\lambda^2}\delta\lambda \tag{3}$$

Comparing the energy shift between σ- and π-transition lines $\delta m_l = 1$ and therefore the value of the Bohr magneton can be determined.

$$\delta E = \mu_B B \Leftrightarrow \mu_B = \frac{\delta E}{B} \tag{4}$$

I.3 Czerny-Turner-spectrometer

A Czerny-Turner-spectrometer will be used to determine the wavelength of the Cadmium line, as the Lummer-Gehrcke-plate only resolves relative wavelengths. The spectrometer uses a diffraction grating to split the incoming light into its spectral lines. The relation between wavelength λ and position p on the camera chip (in the focal plane) can be approximated with a general polynomial function.

$$\lambda(p) = A + B \cdot p + C \cdot p^2 + ... \tag{5}$$

The free parameters are determined by using the calibration spectrum of a lamp with known wavelengths.

I.4 Shape of spectral lines

The CCD-camera of the experimental setup consists of silicon solid state detectors which create a signal out of the incoming light through an internal photoelectric effect. The pixels have a size of $3.6 \times 3.6\mu m$. Then the program ImageJ is used in the evaluation to sum up the intensity values across the vertical axis and create datasets measuring relative intensity versus horizontal placement. The linewidth of the spectral line is determined by several effects. The natural broadening is a result of the uncertainty principle and the finite lifetime of the excited states. It takes the shape of a Lorentzian profile:

$$L(x;\gamma) = \frac{\gamma}{\pi(x^2 + \gamma^2)} \tag{6}$$

Other effects like the thermal Doppler broadening or the influence of the measurement apparatus are better described by a Gaussian.

$$G(x;\sigma) = \frac{1}{\sqrt{2\pi\sigma^2}} \cdot e^{\frac{x^2}{2\sigma^2}} \tag{7}$$

Including all effects the Voigt profile (here centered at zero) gives a precise description of the line shapes:

$$V(x;\sigma,\gamma) = \int_{-\infty}^{\infty} G(x',\sigma) \cdot L(x - x',\gamma)dx' \tag{8}$$

II Determination of the Cadmium wavelength

This is the second part of the experiment but is evaluated at first as the result for the wavelength of the red Cd-line is needed for the evaluation of the first part to determine the Bohr-magneton.
Beside the essential part (the determination of the red Cd-wavelength) our supervisor also provided us images of the spectrum in a range from $\sim$ 590 to 670nm. Thanks to the overlap of these pictures it is possible to merge them together to get one large image (as seen in Figure 2). The resulting spectrum can be compared to the spectrum given in figure 9 of the experiment instructions [1]. One can see that the position of the lines qualitatively is the same. However, as large gaps of areas with no lines cannot be passed, the range that was captured in the experiment is a lot smaller .

To determine the Cd-wavelength an image

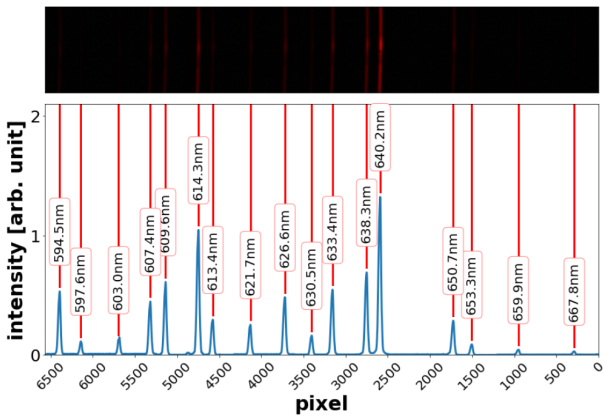

Figure 2: Neon spectrum.
Top: merged images.
Bottom: resulting spectrum with marked spectral lines.

containing the line of interest together with 3 lines of a Neon lamp were taken (Figure 3).

As the wavelengths of the Ne-lamp are known the pixel-scale can be calibrated. In this case a linear relation between λ and the pixels works the best and the Cadmium-wavelength can be determined. The result is plotted in Figure 4.

The result for the wavelength is with

$$\lambda_{Cd} = 643.845 \pm 0.010nm \tag{9}$$

very good. It agrees with the literature value ($\lambda = 643.84695$) [2] in the 1σ-area. The result gets even more impressive regarding the low error of relatively 0.002% which was estimated using the uncertainties of the linear fit and pixel position of the peak.

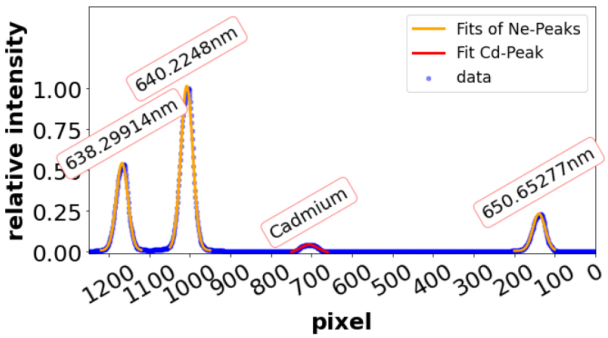

Figure 3: Peak of the Cd-line together with 3 Ne-peaks

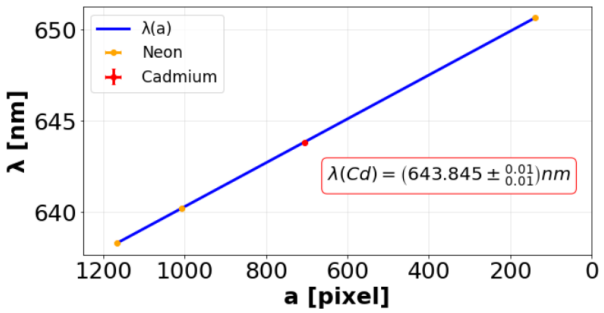

Figure 4: Linear fit through the Neon peaks and determination of the Cd-wavelength

III Determination of the Bohr magneton

With the result of the previous part the Bohr magneton can be determined with the measurements taken with the Lummer-Gehrcke-plate.

III.1 Calibration of the magnet

Beside the exact measurement of the line positions the value with high accuracy of

the magnetic field is essential for good results. In the experiment an electromagnet with ferro magnetic properties is used so it is important to check the hysteresis effect for increasing and decreasing current. This effect is very small as one can see in figure 5. Though one can recognize that the expected linear relation between B and I does not hold for high currents as the ferro magnetic material saturates. That the linear fit is not satisfactory here can also be seen in the pull-distribution: For a good fit all pull-values (residuals normed with the uncertainties) should be between -3 and 3. As the fit clearly does not correspond to the data points the measured values of the B at the specific current I are used in the following evaluation.

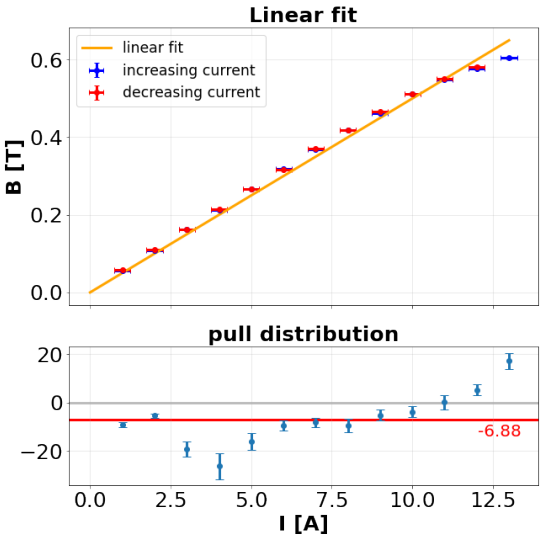

Figure 5: Top: the magnetic field B against the current
Bottom: pull-distribution of the fit

III.2 Determination of $\delta\lambda$

In the transverse direction the σ- and π-lines are visible. By capturing these lines at different currents (different magnetic fields) we get a set of $\delta\lambda$ values that show the shift in wavelength due to the Zeeman effect. To determine this shift, for each of the images taken at $I = 8, 9, 10, 11, 12, 13A$ the peaks of the σ- and π-lines are fitted. This is done by fitting three peaks per time ($\pm\sigma$ and π) with a sum of three individual Voigt functions. A sample plot of this can be seen in Figure 6 taken at $I = 13A$. The orange lines mark the fitted peaks. The fit worked very well here and the errors of the peak positions are smaller than $0.3px$.

By plotting the π-lines against there relative order to each other we can fit a function $k = f(a)$ as it can be seen in Figure 7 for $I = 13A$. This fitted distortion function can be approximated with a second degree polynomial. Having this fit it is possible to determine the orders of the σ-lines and to obtain $\delta k = k_\pi \pm k_\sigma$ for each corresponding triplet. For each of the six measurements corresponding to the currents a mean value for δk is calculated. The error of this value is dominated by the standard deviation of the orders.

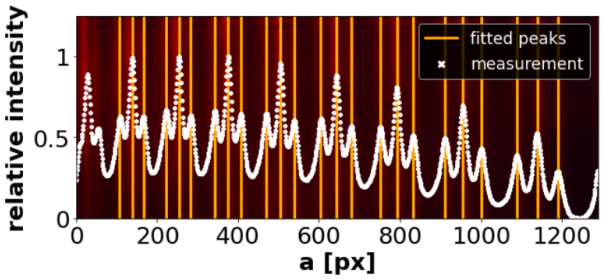

Figure 6: Fit of the peaks on the measurements from the transverse direction for $I = 13A$. In the background: The original image.

To finally calculate the shift $\delta\lambda$ Equation 2 is used. For λ the determined value of II is taken. The values for the thickness

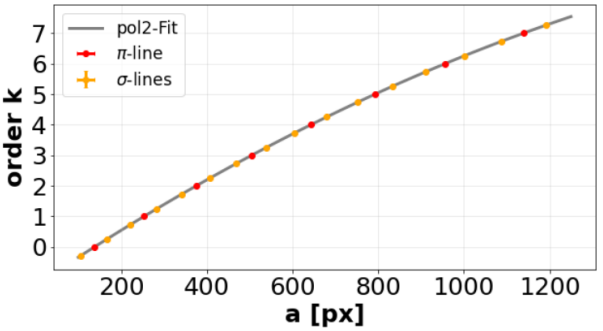

Figure 7: Example fit of $k = f(a)$ for $I = 13A$.

$d = 4.04mm$ of the Lummer-Gehrcke-plate and the indice of refraction $n = 1.4567$ are taken from the instructions [1]. In this calculation the uncertainty of δk is dominating as the value for λ was determined with a very high accuracy.

III.3 Determination of μ_B

Given these shifts in λ the shift in energy δE can be calculated with Equation 1. The uncertainty is once more dominated by $\delta\lambda$.
In the last step μ_B can be determined using Equation 4. Here two approaches are possible:

A μ_B by average

In the first approach μ_B is calculated for each single measurement individually (Equation 4). The final result is given by the average of these values. Again the error is dominated by the standard deviation.

$$\mu_B^{avg} = (9.1 \pm 0.4) \cdot 10^{-24} \frac{J}{T} \qquad (10)$$

B μ_b by linear fit

In the second approach the linear dependency in equation Equation 4 is used to fit a line to the values of δE against the values of B. Referring to this equation the fit is forced to go through the origin. The Bohr magneton simply can be identified with the slope of the fitted line. This leads to a result with a smaller uncertainty:

$$\mu_B^{fit} = (9.11 \pm 0.06) \cdot 10^{-24} \frac{J}{T} \qquad (11)$$

The results agree with each other very well in the 1σ-span. Compared to the literature value $\mu_B = 9.2740100783(28) \cdot 10^{-24} J/T$ [3] the value from the average approach agrees in the 1σ but the uncertainty is with relatively 4.4% much higher than the one of the fit approach (0.7%). Though the second approach value only agrees with the literature value in the 3σ-range.

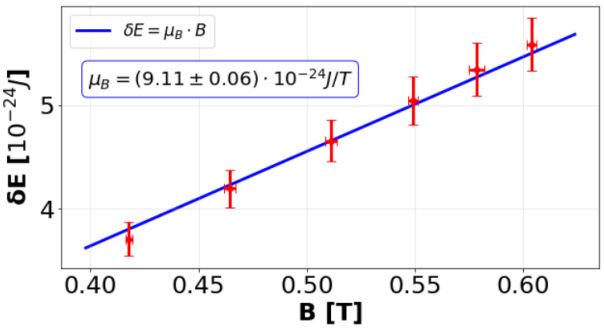

Figure 8: δE against B. The gradient corresponds to the value of the Bohr magneton.

IV Summary and Discussion

At first the polarization of the emitted light was analysed qualitatively. Using polarization filters and $\lambda/4$-waveplates the Zeeman effect could be observed in transversal and longitudinal direction. Here the theory and experimental observations match each other.

Crucial part of this experiment is to determine the Cd-wavelength exactly. This was possible using Czerny-Turner spectrometer. Taking the spectral lines of a Ne-lamp as reference a value of $\lambda = 643.845 \pm 0.010)nm$ was estimated. The uncertainty is very small leaving not much room for any improvements. Of course there could be done multiple measurements for taking the average and a camera with higher resolution would improve the result even more but we do not think that this is needed here.

Taking the result for the Cd-wavelength the Bohr magneton could be determined using the Lummer-Gehrcke plate by varying the strength of the magnetic field. We made two approaches for the final results. First taking the average over the single measurements at the different magnetic strengths, giving us a value of $\mu_B = (9.1 \pm 0.4) \cdot 10^{-24} J/T$. The second approach by fitting a linear curve (δE against B) delivered a much smaller uncertainty: $\mu_B = (9.11 \pm 0.06) \cdot 10^{-24} J/T$. Due to these differences the results agree with the literature value in the 1σ- and 3σ area.

Both approaches are arguable. Nevertheless we think that the average-approach is more robust as the fit-approach only delivers pleasing results if forced to go through the origin. It could be worthy to combine both approaches by taking the average of multiple test series at each magnetic field strength for δE. Then, these results could be used for the fit.
Comparing this result to the measurement of the Cd-wavelength the uncertainties are much larger in this part. This has multiple reasons: The setup is a lot more complex and therefore has more error sources. It starts with measurement of the magnetic field strength. Here it would be of advantage to take the measurements using a smaller step size in the current and to take the measurements at currents/field strengths where the magnet is not in saturation. As before the finite resolution of the camera is a limiting factor as well, but the major problem remains with the quality of the B-field.

All in all the results of this lab are satisfying and it is great to see how it is possible to use relatively simple setups for such precise measurements. We think doing this experiment online works quite good as the important parts are discussed during the meeting. The main task is the evaluation which can be done at home, while the learning effect stays the same.

References

[1] instruction manual: F44 Zeeman effect. `https://www.physi.uni-heidelberg.de/Einrichtungen/FP/versuche/anleitungen.php?lang=en` [2021, April 10]

[2] National Institute of Standards and Technology (NIST). CODATA Recommended Values of the Fundamental Physical Constants 2018.

[3] Kramida, A., Ralchenko, Yu., Reader, J., and NIST ASD Team (2020). NIST Atomic Spectra Database. Available: `https://physics.nist.gov/asd` [2021, April 10].